EUROPEAN JOURNAL OF CANCER 47 (2011) 277–286

available at www.sciencedirect.com

ScienceDirect

journal homepage: www.ejconline.com

Sorafenib tosylate and paclitaxel induce anti-angiogenic, anti-tumour and anti-resorptive effects in experimental breast cancer bone metastases

Maximilian Merz [a], *Dorde Komljenovic* [a], *Stefan Zwick* [b], *Wolfhard Semmler* [a], *Tobias Bäuerle* [a,*]

[a] *Department of Medical Physics in Radiology, German Cancer Research Center, Im Neuenheimer Feld 280, 69120 Heidelberg, Germany*
[b] *Department of Diagnostic Radiology, Medical Physics, University Hospital Freiburg, Hugstetter Str. 55, 79106 Freiburg, Germany*

ARTICLE INFO

Article history:
Received 23 June 2010
Received in revised form 19 August 2010
Accepted 24 August 2010
Available online 20 September 2010

Keywords:
Bone metastases
Angiogenesis
Dynamic contrast-enhanced MRI
Vessel remodelling
Vessel size imaging
Diffusion-weighted imaging
Sorafenib tosylate
Paclitaxel

ABSTRACT

Purpose: In this study we investigated sorafenib tosylate and paclitaxel as single and combination therapies regarding their effects on tumour growth and vasculature as well as their potency to inhibit osteolysis in experimental breast cancer bone metastases.
Experimental design: Nude rats bearing breast cancer bone metastases were treated with sorafenib tosylate (7 mg/kg, $n = 11$), paclitaxel (5 mg/kg, $n = 11$) or the combination of both ($n = 10$) and were compared to untreated controls ($n = 11$). In a longitudinal study, volumes of osteolyses and respective soft tissue tumours were measured in these groups by MRI and volume CT, while changes in cellularity within bone metastases were assessed by diffusion-weighted imaging. Dynamic contrast-enhanced MRI and vessel size imaging was performed to determine changes of tumour vasculature within osseous lesions non-invasively.
Results: Animals treated with sorafenib tosylate or paclitaxel showed significantly reduced growth of both, the osteolytic lesions and the soft tissue tumours as well as a decreased cellularity in bone metastases compared to control rats. Effects on the tumour vasculature of these drugs included significantly reduced blood volume as well as significant changes of the vessel permeability and the mean vessel calibers. When combining sorafenib tosylate with paclitaxel for the treatment of bone metastases positive combination effects were observed, particularly on reducing vessel permeability in these lesions.
Conclusion: The application of sorafenib tosylate monotherapy or in combination with paclitaxel is effective against experimental breast cancer bone metastases resulting in anti-angiogenic, anti-tumour and anti-resorptive effects.

1. Introduction

The skeleton is among the most frequent sites of secondary tumour manifestation in patients suffering from malignant diseases. Evidence for metastatic bone involvement can be found in about 70% of patients dying from breast cancer.[1] Severe complications commonly caused by osteolytic bone lesions include bone pain, hypercalcaemia, pathological fractures and spinal cord compression.[2] Bisphosphonates (BP) are frequently used in patients with breast cancer bone metastases and reduce the frequency of skeletal related events by up to 40%.[3] Although BPs are of major clinical value, bone metastases remain incurable. In addition, some patients become refractory to BPs or suffer from side effects such as renal

* *Corresponding author:* Tel.: +49 6221 422569; fax: +49 6221 422585.
E-mail addresses: t.baeuerle@dkfz.de, t.baeuerle@dkfz-heidelberg.de (T. Bäuerle).
0959-8049/$ - see front matter © 2010 Elsevier Ltd. All rights reserved.
doi:10.1016/j.ejca.2010.08.019

toxicity and osteonecrosis. For these reasons, novel anti-resorptive agents are urgently needed for the treatment of breast cancer patients suffering from metastases to bone.

Angiogenesis plays an important role for the growth of primary tumours and metastases.[4] Proteins including vascular endothelial growth factor (VEGF) are secreted by cancer and stroma cells under low oxygen tensions within a tumour and induce the switch to an angiogenic phenotype.[5] The bone marrow is considered to be a hypoxic environment and breast cancer cells colonising bone depend on the induction of angiogenic signalling.[6] Furthermore, VEGF is directly involved in osteoclastic bone resorption[7] and inhibition of VEGF signalling with bevacizumab as well as sunitinib malate reduces osteolysis and tumour burden in animals bearing experimental bone metastases.[8,9]

Sorafenib tosylate (ST) is a multitargeted receptor tyrosine kinase inhibitor (RTKI) with activities against VEGF receptors 2/3 (VEGFR2/3)[10,11] that to our knowledge ST has not been evaluated for the treatment of bone metastases. ST also inhibits the phosphorylation of mitogen-activated protein (MAP) kinases by Raf in several tumours including breast cancer.[11] By preventing MAP kinase phosphorylation, ST potently interrupts the Ras/Raf/MEK/ERK pathway in cancer cells and demonstrates anti-tumour activities in preclinical xenograft models.[10] ST has already been approved for the treatment of advanced hepatocellular carcinoma and renal cell carcinoma, and the effectiveness of ST alone or in combination with chemotherapy is currently investigated in several clinical trials for different tumour entities.

Dynamic contrast-enhanced magnetic resonance imaging (DCE-MRI) is employed to non-invasively assess changes in blood volume and vessel permeability in tumours under anti-angiogenic therapies in preclinical and clinical settings.[12] Furthermore, changes in the mean vessel size and regional blood volume in tumours due to an anti-angiogenic treatment can be determined by magnetic resonance vessel size imaging (VSI).[13,14] Another non-invasive imaging modality that indicates early treatment response in tumours including prostate cancer bone metastases by detecting changes in cellularity upon treatment is diffusion-weighted MRI (DWI).[12,15]

In the present study, we investigated treatment response to ST as monotherapy and in combination with the taxane paclitaxel in experimental breast cancer bone metastases. To assess the effects of these treatments on angiogenesis, tumour growth and bone resorption, we applied non-invasive imaging techniques including DCE-MRI, VSI and DWI and combined results with findings from morphologic MRI and volumetric computed tomography (VCT) in a longitudinal *in vivo* study.

2. Materials and methods

2.1. Cell culture

The human mammary adenocarcinoma cell line MDA-MB-231 was purchased from the American Type Culture Collection and cultured routinely in RPMI-1640 (Invitrogen, Karlsruhe, Germany) supplemented with 10% (v/v) FCS (Sigma, Taufkirchen, Germany). All cultures were maintained in a humidified atmosphere of 5% CO_2 at 37 °C and passaged 2–3 times a week to keep them in logarithmic growth.

2.2. Animal model and treatment

Experiments were approved by the governmental review committee on animal care (Regierungspräsidium Karlsruhe, Germany). Nude rats (RNU strain) were obtained from Harlan Winkelmann GmbH (Borchen, Germany) at the age of 6 weeks and housed in a mini-barrier system under specific pathogen-free conditions.

For tumour cell inoculation, subconfluent MDA-MB-231 cells were trypsinised and resuspended in RPMI-1640 to a final concentration of 10^5 cells/200 μl. Animals were anaesthetised with a mixture of nitrous oxide (1 l/min), oxygen (0.5 l/min) and isofluran (1.5 vol.%), and 10^5 MDA-MB-231 cells were injected into the superficial epigastric artery as described earlier.[16] Resulting bone metastases were observed exclusively in the femur, tibia and fibula of the respective leg.

Thirty days after tumour cell inoculation initial imaging was performed and animals ($n = 43$) were randomly assigned into a control group and three therapy groups. Animals of the therapy groups received either ST (Bayer Pharmaceuticals Corporation, West Haven, CT; $n = 11$; oral application of 7 mg/kg, daily), paclitaxel (Paclitaxel HEXAL, Hexal AG, Holzkirchen, Germany; $n = 11$; intraperitoneal application of 5 mg/kg, weekly) or a combination therapy of both ($n = 10$; 7 mg/kg of ST, daily oral application and 5 mg/kg of paclitaxel, intraperitoneal application, weekly). Therapeutics were applied until day 55 after tumour cell inoculation and treated rats were compared to sham-treated controls ($n = 11$).

2.3. In vivo imaging

All animals were imaged on days 30, 35, 45 and 55 after tumour inoculation in an experimental flat-panel detector equipped volume CT (Volume CT, Siemens, Germany) and a clinical 1.5 T MRI (Symphony, Siemens, Germany) using a home-built coil for radiofrequency excitation and detection. VSI was performed at days 30 and 55 after tumour cell inoculation. For all examinations, animals were anaesthetised with the same mixture of nitrous oxide, oxygen and isofluran as used for tumour cell injection.

2.3.1. Volumetric computed tomography

VCT was performed with the following parameters: tube voltage 80 kV, tube current 50 mA, scan time 51 s, rotation speed 10 s, 120 frames/s, matrix 512×512 and slice thickness 0.2 mm.

2.3.2. Magnetic resonance imaging

(1) *T2-weighted images*: turbo spin echo sequence (orientation axial, TR 3240 ms, TE 81 ms, matrix 152×256, resolution $0.35 \times 0.35 \times 1.5$ mm^3, 3 averages, 15 images, scan time 3:40 min).
(2) *Diffusion-weighted imaging*: half-Fourier acquisition single-shot turbo spin echo sequence (HASTE; $b = 0$, 50, 100, 200, and 600 s/mm^2 through the largest diameter of the tumour, orientation axial, TR 4000 ms, TE

155 ms, matrix 72×128, resolution $0.96 \times 0.96 \times 2.0$ mm^3, 10 averages, 15 images, scan time $5 \times 2{:}00$ min).

(3) *Dynamic contrast-enhanced imaging*: saturation recovery turbo FLASH (fast low angle shot) sequence (through the largest diameter of the tumour, orientation axial, TR 373 ms, TE 1.86 ms, T_{REC} 130 ms, flip angle 20°, matrix 192×144, resolution $0.78 \times 0.78 \times 5.0$ mm^3, 1 average, 512 images, scan time 6:55 min) while infusing intravenously 0.1 mmol/kg Gd-DTPA (Magnevist, Schering, Germany) over a time period of 10 s.

(4) *Vessel size imaging*: T2-weighted spin echo sequences (TR 6000 ms, TE 80 ms, matrix 128×104, resolution $0.5 \times 0.5 \times 1.5$ mm^3, 1 average, 12 images, scan time $2 \times 13{:}00$ min) and T2*-weighted multi gradient echo sequences (FLASH, TR 320 ms, TE 4.76–47.6 ms, matrix 128×104, resolution $0.5 \times 0.5 \times 1.5$ mm^3, 3 averages, 12 images, scan time $2 \times 7{:}00$ min) were acquired before and 3 min after intravenous administration of ultra small paramagnetic iron oxide particles (USPIO; 200 μmol Fe/kg; Sinerem, Laboratoires Guerbet, Aulnay-sous-Bois, France). Due to technical problems five animals of the control group and ST monotherapy group had to be excluded from postprocessing on day 30.

2.3.3. Postprocessing

Volumes [μl] of the osteolytic lesion (OL) and the respective soft tissue component (SC) were determined by analysing unenhanced VCT and T2-weighted MR images respectively with the Medical Imaging Interaction Toolkit (MITK, Heidelberg, Germany). For DCE-MRI, VSI and DWI regions of interest were drawn manually around the tumour to quantify the following parameters. Data from DCE-MRI was analysed according to the pharmacokinetic two-compartment model of Brix and colleagues[17] using the Dynalab workstation (Fraunhofer Mevis, Bremen, Germany) to calculate *amplitude A* ([arbitrary units], associated with relative blood volume) and *exchange rate constant* k_{ep} ([1/min], reflecting vessel permeability). Vessel size imaging data was analysed according to the model introduced by Tropres and colleagues[13] using a custom-built software created with RadBuilder (Siemens Corporate Research, Princeton, NJ) to determine parameters *vessel size index VI* ([μm], reflecting the mean vessel diameter within bone metastases) and *regional blood volume BV* [arbitrary units]. Maps for the *apparent-diffusion coefficient ADC* ([mm^2/s $\times 10^{-5}$], correlating negatively with cell density[18]) were acquired with the DWI stat module (in house software, cooperation with Fraunhofer Mevis, Bremen, Germany).

2.4. Bone storage and histology

Bone metastases were resected on day 55 after tumour cell inoculation and processed as described previously.[9] Immunostaining of 5 μm thick sections was performed overnight at 4 °C using a rabbit anti-rat collagen IV antibody (Progen Biotechnik GmbH, Heidelberg, Germany) in combination with a Texas Red-conjugated donkey anti-rabbit antibody (Jackson Immunoresearch, Suffolk, UK). Smooth muscle actin (SMA) was stained with a mouse anti-rat antibody (Sigma–Aldrich, Saint Louis, MO) in combination with a Cy2-conjugated goat anti-mouse antibody (Jackson Immunoresearch, Suffolk, UK). Cell nuclei were counterstained with DAPI (Serva, Germany). Control sections omitted primary antibodies and showed no staining signal.

A Leica microscope (DMRE, Bensheim, Germany) with an adapted digital camera (F-view XS, Soft Imaging System, Muenster, Germany) was used to examine five fields of view of fluorescence stainings from five representative animals of each group. To quantify marker densities on these histological sections positive area fractions (PAF) were determined with the Analysis Software (cell^F, Olympus Soft Imaging Solutions, Germany). The mean PAF of collagen IV were determined to characterise tumour vascularisation in bone metastases. On the same sections mean vessel calibers were determined by measuring diameters of orthogonally cut vessels. Tangentially cut vessels were excluded from counting.

2.5. Statistical analyses

For statistical comparisons, the respective absolute values for imaging parameters OL, SC, A, k_{ep}, *VI*, *BV* and *ADC* as well as PAF and mean vessel calibers from histological analysis were compared between the control and treatment groups using the two-sided Wilcoxon-test; p-values < 0.05 were considered significant.

3. Results

3.1. ST and paclitaxel reduce growth of osteolytic lesions and the respective soft tissue tumours in bone metastases as imaged with VCT and MRI

In general, treatment with ST, paclitaxel or the combination therapy was well tolerated and no animals died during the observation period or showed signs for significant weight loss. In untreated animals volumes for both, the OL and SC increased during the observation period, as compared to initial values at day 30 after tumour cell inoculation (Figs. 1A and B & 2; Table 1). After monotherapy with ST a significant reduction of the OL volume was observed on days 45 and 55 and of the SC volume on day 55 in comparison to untreated animals ($p < 0.05$; Figs. 1A and B & 2; Table 1). Animals treated with paclitaxel showed significantly decreased OL volumes from day 35 to 55 compared to controls ($p < 0.05$, day 35; $p < 0.01$, day 45 and 55; Figs. 1A and B & 2; Table 1) while significantly smaller SC values were measured on days 45 ($p < 0.05$) and 55 ($p < 0.01$). The combination of ST and paclitaxel resulted in a significant reduction of OL volumes from day 35 to 55 ($p < 0.05$, day 35; $p < 0.01$, day 45 and 55). Furthermore, a significant reduction of the SC volumes was measured on days 45 and 55 ($p < 0.01$, days 45 and 55; Figs. 1A and B & 2; Table 1).

3.2. ST and paclitaxel induce changes of DCE-MRI parameter amplitude and show positive combination effects on the exchange rate constant

Compared to controls, bone metastases treated with ST as single agent showed significantly decreased values for *A*

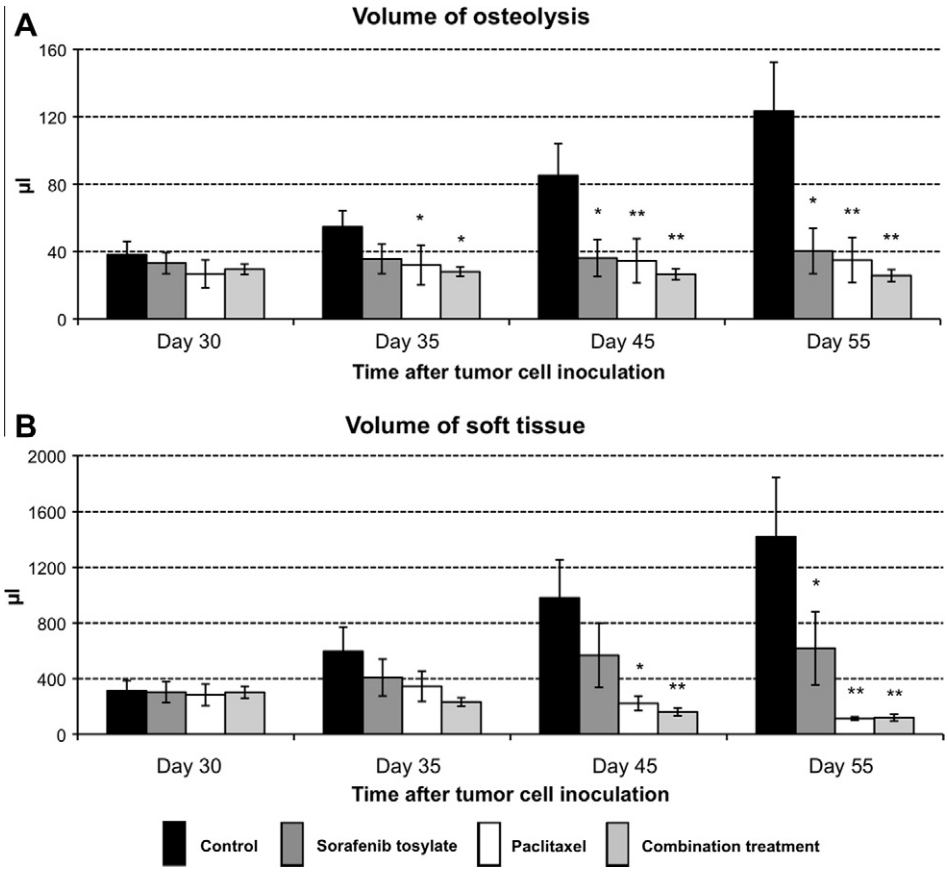

Fig. 1 – Results of parameters acquired with VCT and MRI between day 30 and 55 after tumour cell inoculation in animals bearing breast cancer bone metastases. (A) Volumes of the osteolytic lesions as imaged with VCT and (B) volumes of the soft tissue components as imaged with T2-weighted MRI. All values are presented as mean values. Error bars indicate standard errors; asterisks denote a significant difference between the groups ($^{*}p < 0.05$; $^{**}p < 0.01$).

and k_{ep} from day 35 to 55 (A: $p < 0.01$; k_{ep} $p < 0.01$ on days 35 and 55; $p < 0.05$ on day 45; Figs. 3A and B & 4A; Table 1). Significantly decreased values for *A* were also found in animals treated with paclitaxel from day 45 ($p < 0.05$) to 55 ($p < 0.01$) while higher values for k_{ep} were measured from day 35 until day 55, reaching significance only on day 35 ($p < 0.05$; Figs. 3A and B & 4A; Table 1). When comparing animals treated with the combination therapy to controls, significantly reduced values for *A* and k_{ep} were found from day 35 to 55 ($p < 0.01$).

3.3. *ST and paclitaxel reduce regional blood volume and change vessel size indices in bone metastases as demonstrated with VSI*

Comparing animals treated with ST, paclitaxel or the combination therapy with controls, significantly reduced *BV* values were assessed on day 55 after tumour cell inoculation ($p < 0.01$; Figs. 3C and 4B; Table 1). Compared to the control group, in animals receiving ST or the combination therapy also significantly enlarged mean vessel calibers within bone metastases were observed ($p < 0.01$; Figs. 3C and 4B; Table 1), whereas decreased *VI* were found in bone metastases of rats treated with paclitaxel on day 55 ($p < 0.05$).

3.4. *ST and paclitaxel increase apparent-diffusion coefficients within experimental bone metastases as assessed by DWI*

DWI showed significantly increased *ADC* values in tumours treated with ST on day 45 ($p < 0.05$) and 55 ($p < 0.01$) compared to controls (Figs. 3D and 4B; Table 1). Under monotherapy with paclitaxel higher *ADC* values compared to controls were measured on day 55 ($p < 0.05$; Figs. 3D and 4B; Table 1). Significantly higher *ADC* values within bone metastases of animals treated with the combination therapy were observed on days 45 and 55 in comparison to untreated animals ($p < 0.01$; Figs. 3D and 4B; Table 1).

3.5. *Immunohistological analysis of bone metastases*

Immunohistological analysis of bone metastases from untreated control animals revealed tortuous vessels of irregular shape and caliber as indicated by collagen IV staining. Especially vessels of larger diameters in these bone metastases were co-localised with SMA-positive cells (Fig. 5A). In all treated animals a significantly reduced PAF for collagen IV compared to the control group was observed ($p < 0.01$; Fig. 5B–D; Table 1) whereas no significant differences between

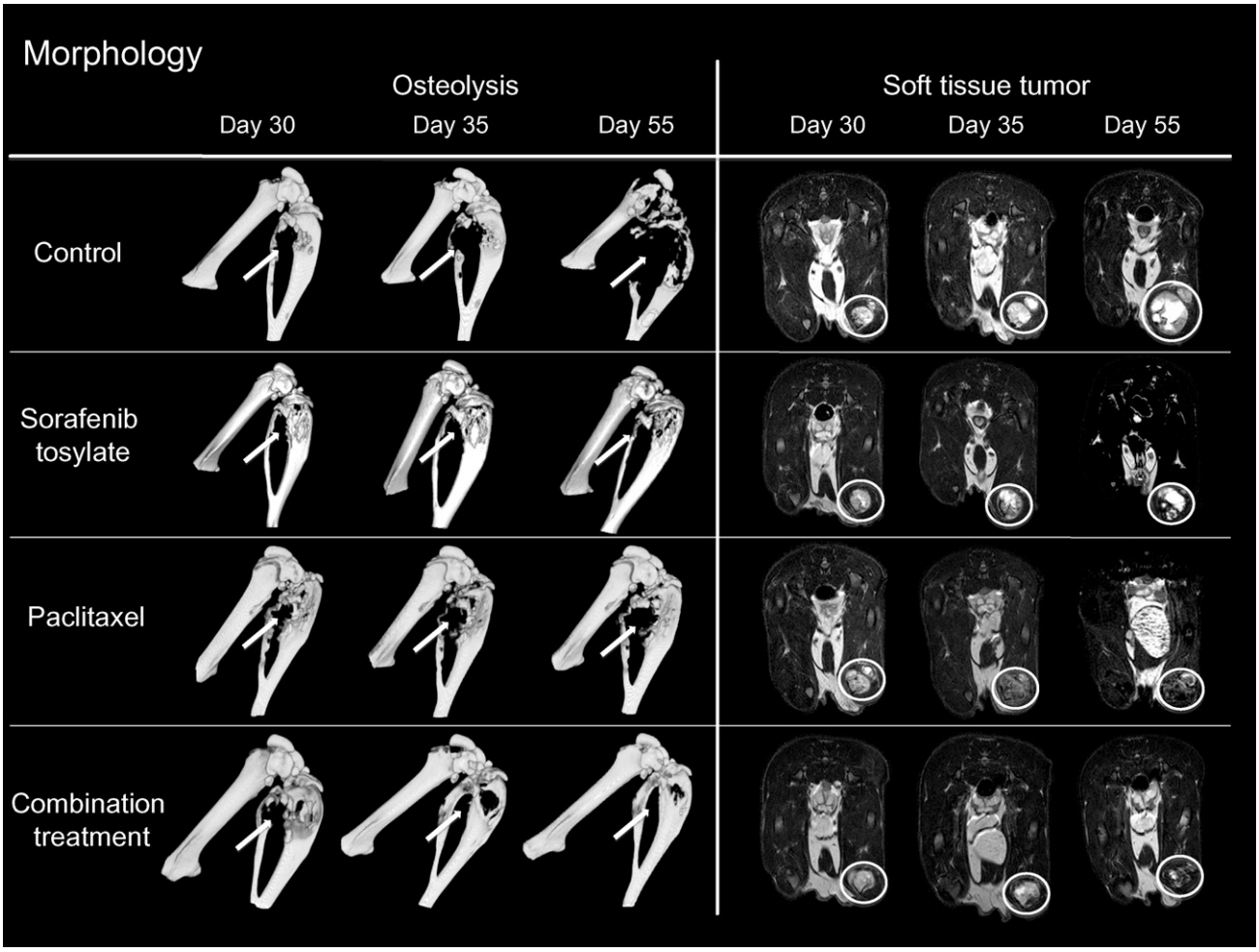

Fig. 2 – Morphology of bone metastases as imaged with VCT and MRI on days 30, 35 and 55 after tumour cell inoculation. Left side: 3D surface reconstructions from VCT images (white arrows indicating osteolyses within bones of the right hind leg). Right side: axial slices from T2-weighted MRI through the largest diameter of the hyperintense soft tissue tumour (delineated by white circles in each row).

the groups were found for SMA-positive area fractions ($p > 0.05$; Fig. 5B–D; Table 1). Bone metastases treated with ST or the combination therapy also showed a significantly reduced ratio of collagen IV/SMA-positive area fractions ($p < 0.01$; Fig. 5B and D; Table 1) while in paclitaxel treated animals no significant differences were found. Furthermore, animals treated with ST or the combination therapy showed significantly enlarged mean vessel diameters compared to untreated tumours ($p < 0.01$; Fig. 5B and D; Table 1) whereas treatment with paclitaxel resulted in significantly reduced mean vessel calibers compared to untreated controls ($p < 0.01$; Fig. 5C; Table 1).

3.6. *Comparison between the groups*

Treatment with the combination therapy resulted in a significant reduction of the DCE-MRI parameter k_{ep} when compared to the respective values from both, animals treated with either ST or paclitaxel on days 45 ($p < 0.01$) and 55 ($p < 0.05$; Figs. 3A and B & 4A; Table 1). Otherwise, comparison of treatment groups did not result in significant differences for *in vivo* imaging and immunohistochemical analysis ($p > 0.05$, respectively). However, combination of ST and paclitaxel resulted in positive, but non-significant treatment effects in comparison to the respective monotherapies, particularly for the volume of osteolysis and the DCE-MRI parameter *A* at each time point of the observation period (Figs. 1A and 3A; Table 1).

4. Discussion

Our aim was to non-invasively assess treatment response of experimental breast cancer bone metastases to ST and paclitaxel as single and combination therapies using morphological and functional imaging techniques in a longitudinal *in vivo* study.

Anti-tumour effects of ST were revealed by T2-weighted MRI and DWI as treated animals showed significantly reduced volumes of the soft tissue components as well as higher *ADC* values indicating a decreased cell density within bone metastases. In addition to these anti-tumour properties, we observed anti-resorptive effects of ST by VCT analysis of bone

Table 1 – Study results. For *in vivo* experiments all mean values from days 30, 35, 45 and 55 are given in absolute numbers ± standard error. For histology, values for collagen IV and smooth muscle actin (SMA) are expressed as positive area fractions (PAF) in percent, vessel diameters are given as mean values in μm. Asterisks denote a significant difference between groups ($^{*}p < 0.05$; $^{**}p < 0.01$).

In vivo		Day 30	Day 35	Day 45	Day 55
fpVCT: Osteolysis (μl)	Control	38 ± 8	54 ± 10	85 ± 20	123 ± 30
	Sorafenib tosylate	33 ± 6	35 ± 9	36 ± 11*	40 ± 13*
	Paclitaxel	26 ± 8	32 ± 12*	34 ± 13**	35 ± 13**
	Combination treatment	29 ± 3	28 ± 3*	26 ± 3**	25 ± 4**
MRI: Soft tissue tumour (μl)	Control	311 ± 77	596 ± 182	981 ± 286	1420 ± 445
	Sorafenib tosylate	302 ± 75	407 ± 132	567 ± 231	617 ± 263*
	Paclitaxel	283 ± 77	344 ± 109	222 ± 52*	111 ± 13**
	Combination treatment	301 ± 43	232 ± 30	160 ± 28**	119 ± 24**
DCE-MRI: Amplitude *A* (a.u.)	Control	1.06 ± 0.04	1.08 ± 0.04	1.10 ± 0.06	1.09 ± 0.05
	Sorafenib tosylate	1.14 ± 0.05	0.89 ± 0.03**	0.85 ± 0.04**	0.78 ± 0.04**
	Paclitaxel	1.01 ± 0.02	1.02 ± 0.05	0.86 ± 0.05*	0.81 ± 0.03**
	Combination treatment	1.08 ± 0.03	0.83 ± 0.03**	0.77 ± 0.05**	0.75 ± 0.04**
DCE-MRI: Exchange rate constant k_{ep} (1/min)	Control	51 ± 4	49 ± 5	53 ± 7	47 ± 6
	Sorafenib tosylate	54 ± 6	23 ± 3**	34 ± 4*	29 ± 2**
	Paclitaxel	53 ± 3	60 ± 3*	58 ± 4	54 ± 4
	Combination treatment	53 ± 5	29 ± 4**	19 ± 2**	21 ± 2**
VSI: Blood volume (a.u.)	Control	290 ± 19	–	–	332 ± 6
	Sorafenib tosylate	320 ± 37	–	–	231 ± 16**
	Paclitaxel	324 ± 13	–	–	238 ± 15**
	Combination treatment	309 ± 10	–	–	244 ± 13**
VSI: Vessel size index (μm)	Control	47 ± 6	–	–	43 ± 3
	Sorafenib tosylate	43 ± 5	–	–	69 ± 4**
	Paclitaxel	43 ± 3	–	–	32 ± 4*
	Combination treatment	41 ± 4	–	–	66 ± 7**
DWI: *ADC* ($mm^2/s \times 10^{-5}$)	Control	114 ± 10	114 ± 9	90 ± 8	91 ± 9
	Sorafenib tosylate	109 ± 6	122 ± 12	132 ± 17*	145 ± 14**
	Paclitaxel	102 ± 4	98 ± 8	101 ± 7	123 ± 4*
	Combination treatment	104 ± 3	114 ± 7	130 ± 12**	147 ± 13**
Ex vivo		Collagen IV	SMA	Collagen IV/SMA	Vessel diameter
Histology	Control	3.68 ± 1.44	1.07 ± 0.59	3.44 ± 2.33	9.86 ± 3.36
	Sorafenib tosylate	1.35 ± 0.43**	0.98 ± 0.54	1.38 ± 0.88**	15.02 ± 8.40**
	Paclitaxel	2.39 ± 0.48**	0.88 ± 0.21	2.72 ± 0.85	8.66 ± 3.30**
	Combination treatment	1.45 ± 0.53**	0.80 ± 0.28	1.81 ± 0.92**	15.40 ± 6.89**

destruction. Our group recently showed that anti-angiogenic effects including vessel remodelling in breast cancer bone metastases after VEGFR inhibition preceded anti-tumour and anti-resorptive effects in these lesions.[9] Correspondingly, anti-angiogenic properties of ST could explain the observed anti-tumour and anti-resorptive effects in our study as reported before for the treatment of experimental bone metastases with bevacizumab and sunitinib malate.[8,9]

Upon ST treatment, anti-angiogenic effects have been demonstrated by Wilhelm and colleagues resulting from an inhibition of VEGFR2/3 RTK phosphorylation, which reduced the microvessel density in different tumour xenografts.[11] Our results from DCE-MRI and VSI are in good agreement with these observations as significantly lower values for parameters *A*, k_{ep} and *BV* were found in animals treated with ST reflecting a reduction in blood volume and vessel permeability.[19] Compared to the control group also significantly enlarged mean vessel calibers within tumours were measured with VSI upon ST treatment. Histological analysis confirmed these findings and furthermore showed an increased co-localisation of collagen IV and SMA on tumour vessels indicating vascular remodelling within bone metastases. This might result from the disruption of predominantly smaller and immature vessels within the tumour, which are more susceptible to anti-angiogenic therapy.[20] Our findings from histology support this hypothesis, as the increased fractional coverage of tumour blood vessels by SMA-positive cells was primarily due to the reduction of collagen IV and not resulting from an increase of SMA expression. Interestingly, a recent study demonstrated that small capillaries close to the bone surface are responsible for the distribution of osteoclast precursor cells to bone remodelling units.[21] Therefore the ablation of these smaller vessels by ST could lead to the reduction of bone resorption. Taken together, results from

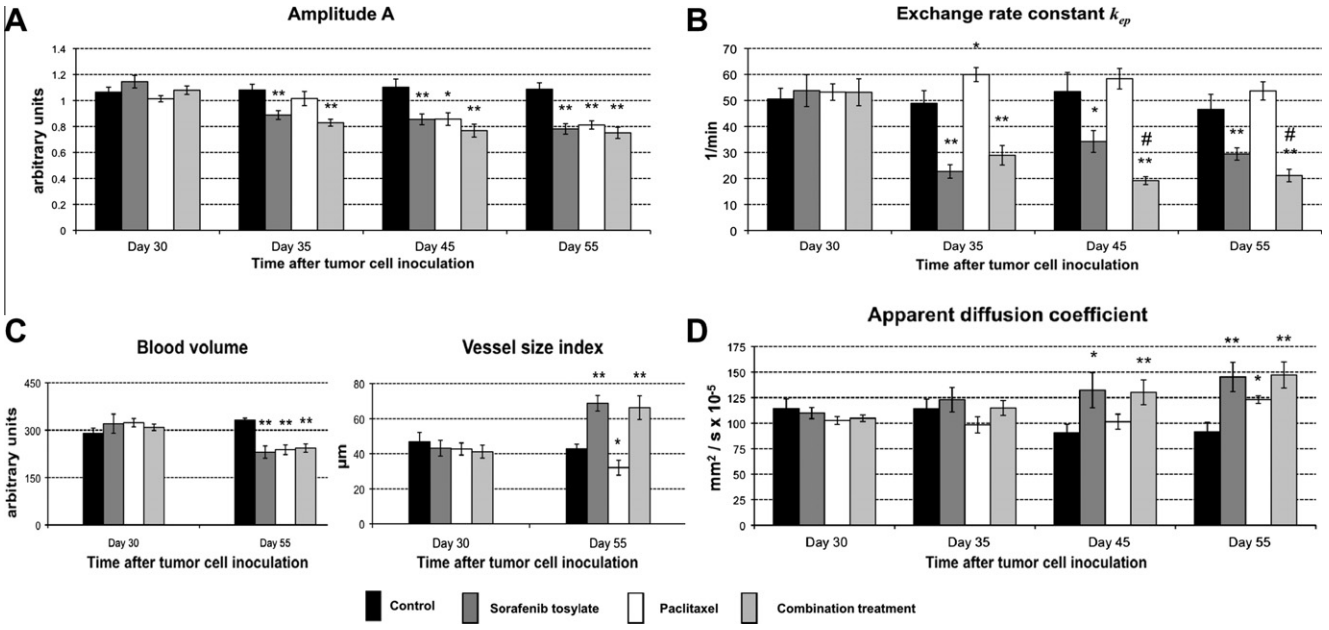

Fig. 3 – Results of parameters acquired with DCE-MRI, VSI and DWI between day 30 and 55 after tumour cell inoculation in animals bearing breast cancer bone metastases. (A) Amplitude *A* (DCE-MRI); (B) exchange rate constant k_{ep} (DCE-MRI); (C) regional blood volume and vessel size index (VSI); and (D) apparent diffusion coefficient *ADC* (DWI). All values are presented as mean values. Error bars indicate standard errors; asterisks denote a significant difference between groups ($^{*}p < 0.05$; $^{**}p < 0.01$; and $^{\#}p < 0.05$ for combination treatment versus paclitaxel and sorafenib tosylate monotherapy groups).

non-invasive imaging and histology indicated an inhibition of angiogenesis including vascular remodelling in bone metastases upon ST treatment.

Besides the inhibition of angiogenesis, the disruption of the Ras/Raf/MEK/ERK pathway in osteoclasts by ST might have contributed to the observed anti-resorptive effects. The anti-resorptive properties of nitrogen-containing bisphosphonates (NBP) are primarily based on the interference with the mevalonate pathway and the prevention of the post-translational modification of small GTP-binding proteins including Ras,[22] and consequently interrupting the Raf kinase cascade.[23] This suggests that inhibition of Raf kinases by ST could parallel the mode of action of NBPs, but this hypothesis has to be confirmed in further experimental studies.

The treatment with paclitaxel resulted in decreased volumes for osteolyses and the respective soft tissue tumours of experimental bone metastases as imaged with VCT and T2-weighted MRI. In addition, higher *ADC* values within osseous lesions were measured with DWI. Similar results have been shown for paclitaxel in a recent study investigating its use in bone metastases compared to a novel microtubule-binding agent (MBA).[24] In this study, the authors attributed the inhibition of osteoclast activity to direct cytotoxic effects on these cells. Our results suggest that the anti-resorptive properties of paclitaxel could be explained by its anti-angiogenic effects. With DCE-MRI and VSI we showed that paclitaxel increased vessel permeability and reduced blood volume as well as mean vessel calibers within bone metastases. MBAs like paclitaxel inhibit tumour neo-vascularisation by impeding endothelial cell proliferation, migration, and tube formation.[25] Furthermore, MBAs act as vascular disrupting agents on larger pre-existing vessels by interfering with focal adhesions and adherens junctions on endothelial cells.[26] This might explain our findings of reduced blood volume and smaller mean vessel calibers in experimental bone metastases that were accompanied by increased vessel permeability in paclitaxel treated tumours.

The comparison between groups receiving ST or paclitaxel as single agents shows that anti-tumour properties of paclitaxel were stronger to those of ST while anti-angiogenic effects were more pronounced in animals treated with the RTKI. The differences between both agents regarding their effects on tumour vascularisation and morphology were the rationale of combining both treatments. Furthermore, preclinical and clinical studies showed that combining anti-angiogenic agents with cytotoxic chemotherapies like paclitaxel had beneficial effects.[27,28] In line with this observation, combined use of ST and paclitaxel resulted in enhanced anti-resorptive and anti-angiogenic effects when compared to the respective monotherapies, although significant differences between these groups were only found for the DCE-MRI parameter k_{ep}. It can be concluded, that the observed decrease in vessel permeability upon combination treatment as indicated by k_{ep} is important for the induction of a more laminar flow in tumour vessels and therefore increases local drug distribution in these lesions.[29]

However, based on our results ST is not superior to paclitaxel for the treatment of experimental breast cancer bone metastases when used as monotherapies. Nevertheless, alternative treatments are needed for patients with breast cancer bone metastases, who suffer from severe side effects or become refractory to standard treatments including NBP or

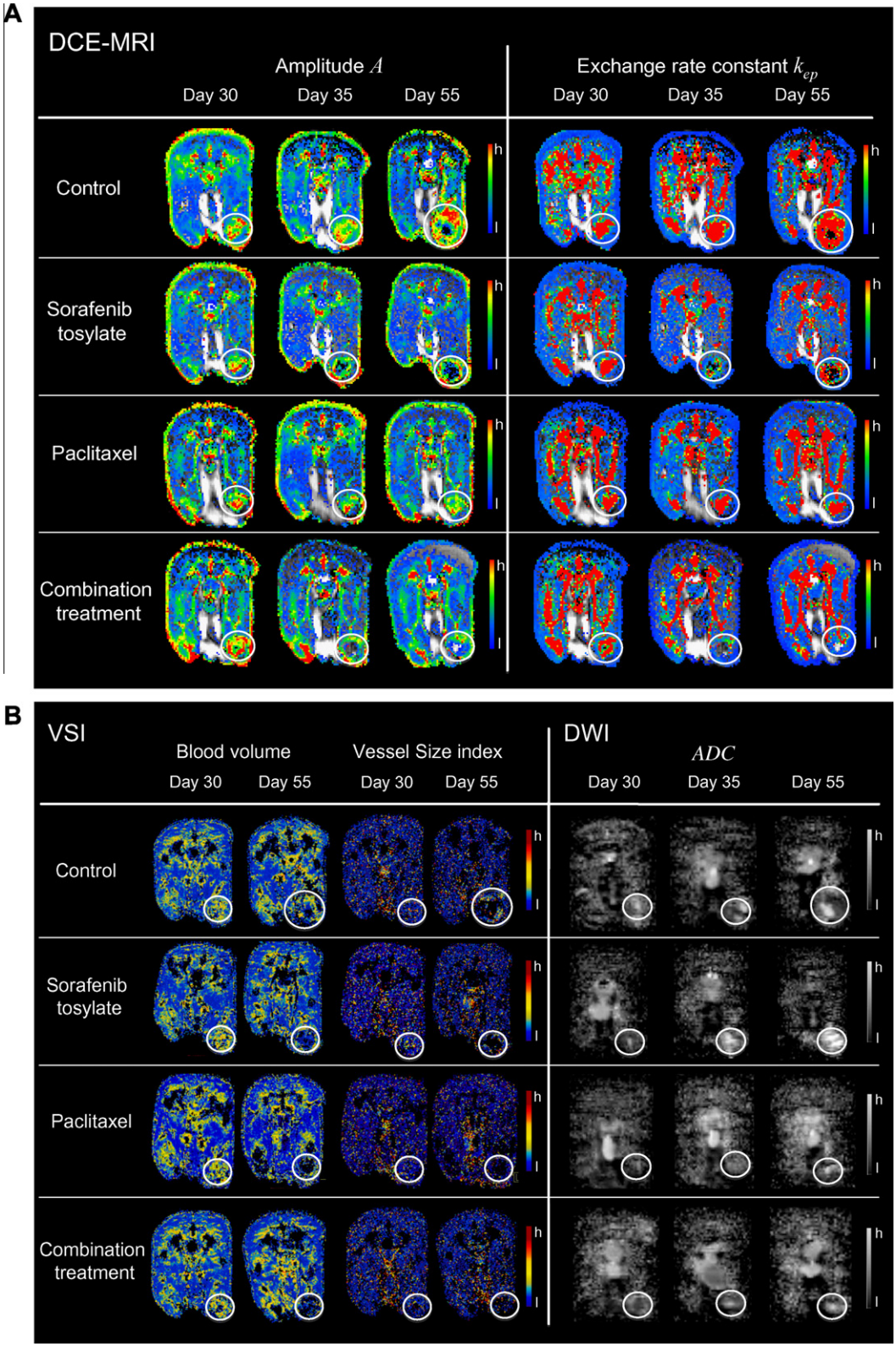

Fig. 4 – Colour maps of experimental breast cancer bone metastases as imaged by DCE-MRI, VSI and DWI. (A) DCE-MRI colour maps of amplitude *A* (left side) and exchange rate constant k_{ep} (right side) on days 30, 35 and 55 after tumour cell inoculation with values ranging from high (h) in red to low (l) in blue. (B) VSI colour maps of blood volume and vessel size index (left side) on days 30 and 55 after tumour cell inoculation ranging from high (h) values in red to low (l) values in blue. *ADC* maps from DWI (right side) on days 30, 35 and 55 after tumour cell inoculation ranging from high (h) values in white to low (l) values in black. All maps are presented in axial orientation; white circles delineate bone metastases.

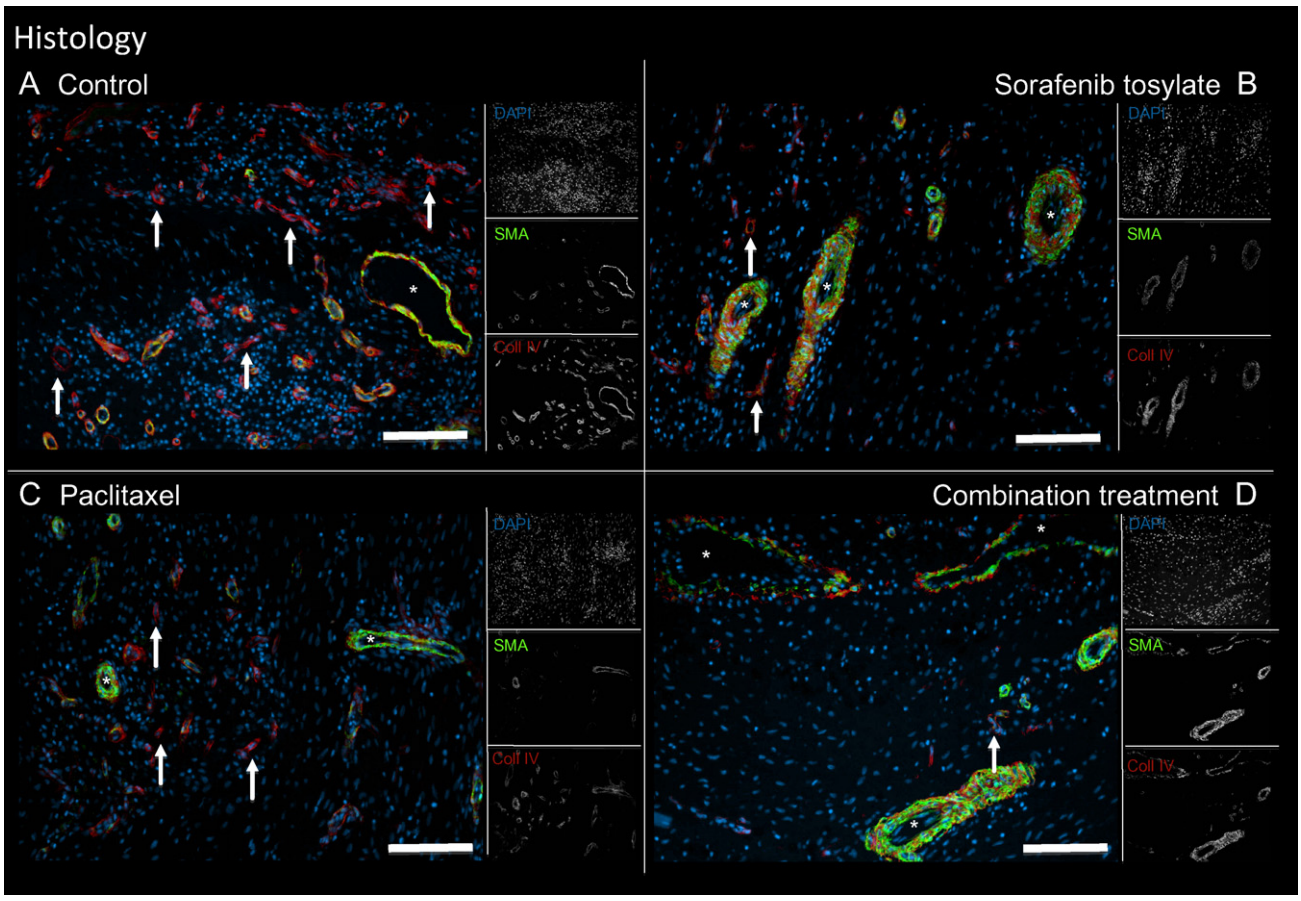

Fig. 5 – Immunohistological stainings of experimental breast cancer bone metastases from a representative animal of each group (A: Control, B: Sorafenib tosylate, C: Paclitaxel, and D: Combination treatment). Coloured images show merged single channels (single channels shown on the right of each merged image) for DAPI (blue), SMA (green) and collagen IV (Coll IV, red). Arrows point at small vessels negative for SMA, asterisks indicate SMA/collagen IV co-localised vessels. Magnification: 20 fold; bar: 100 μm.

conventional chemotherapeutics such as paclitaxel. Under these circumstances ST might be a promising alternative to the use of standard therapies as it exhibited anti-angiogenic, anti-tumour and anti-resorptive effects by using a different mode of action as compared to NBP or paclitaxel.

In conclusion, our results show that ST alone or in combination with paclitaxel is effective against experimental breast cancer bone metastases. Further studies with different doses and administration schedules of the combination partners are needed to optimise treatment effects and clinical trials will show whether the observed effects are applicable to treat patients suffering from metastasis to bone.

Financial support

Tobias Bäuerle and Dorde Komljenovic (Deutsche Forschungsgemeinschaft, SFB-TR23).

Support of drugs

Sorafenib tosylate from Bayer Schering Pharma; Sinerem from Guerbet.

Conflict of interest statement

None declared.

Acknowledgements

We thank Karin Leotta and Renate Bangert for excellent technical assistance as well as Bram Stieltjes, Frederik Laun and Dirk Simon for their support and valuable discussions about DWI techniques. We furthermore thank Bayer Schering Pharma for providing Sorafenib tosylate, Guerbet for supplying Sinerem and the Deutsche Forschungsgemeinschaft (SFB-TR23) for their financial support.

REFERENCES

1. Plunkett TA, Smith P, Rubens RD. Risk of complications from bone metastases in breast cancer. Implications for management. *Eur J Cancer* 2000;**36**(4):476–82.

2. Coleman RE. Clinical features of metastatic bone disease and risk of skeletal morbidity. *Clin Cancer Res* 2006;**12**(20 Pt):6243s–9s.
3. Body JJ. Breast cancer: bisphosphonate therapy for metastatic bone disease. *Clin Cancer Res* 2006;**12**(20 Pt 2):6258s–63s.
4. Folkman J. Role of angiogenesis in tumor growth and metastasis. *Semin Oncol* 2002;**29**(6 Suppl 16):15–8.
5. Folkman J. Seminars in Medicine of the Beth Israel Hospital, Boston. Clinical applications of research on angiogenesis. *New Engl J Med* 1995;**333**(26):1757–63.
6. Dunn LK, Mohammad KS, Fournier PG, et al. Hypoxia and TGF-beta drive breast cancer bone metastases through parallel signaling pathways in tumor cells and the bone microenvironment. *PLoS One* 2009;**4**(9):e6896.
7. Nakagawa M, Kaneda T, Arakawa T, et al. Vascular endothelial growth factor (VEGF) directly enhances osteoclastic bone resorption and survival of mature osteoclasts. *FEBS Lett* 2000;**473**(2):161–4.
8. Bäuerle T, Hilbig H, Bartling S, et al. Bevacizumab inhibits breast cancer-induced osteolysis, surrounding soft tissue metastasis, and angiogenesis in rats as visualized by VCT and MRI. *Neoplasia* 2008;**10**(5):511–20.
9. Bäuerle T, Merz M, Komljenovic D, Zwick S, Semmler W. Drug induced vessel remodeling in bone metastases as assessed by dynamic contrast enhanced MRI and vessel size imaging – a longitudinal *in vivo* study. *Clin Cancer Res* 2010;**16**(12):3215–25.
10. Wilhelm S, Carter C, Lynch M, et al. Discovery and development of sorafenib: a multikinase inhibitor for treating cancer. *Nat Rev Drug Discov* 2006;**5**(10):835–44.
11. Wilhelm SM, Carter C, Tang L, et al. BAY 43-9006 exhibits broad spectrum oral antitumor activity and targets the RAF/MEK/ERK pathway and receptor tyrosine kinases involved in tumor progression and angiogenesis. *Cancer Res* 2004;**64**(19):7099–109.
12. Jain RK, Duda DG, Willett CG, et al. Biomarkers of response and resistance to antiangiogenic therapy. *Nat Rev Clin Oncol* 2009;**6**(6):327–38.
13. Tropres I, Grimault S, Vaeth A, et al. Vessel size imaging. *Magn Reson Med* 2001;**45**(3):397–408.
14. Zwick S, Strecker R, Kiselev V, et al. Assessment of vascular remodeling under antiangiogenic therapy using DCE-MRI and vessel size imaging. *J Magn Reson Imaging* 2009;**29**(5):1125–33.
15. Lee KC, Sud S, Meyer CR, et al. An imaging biomarker of early treatment response in prostate cancer that has metastasized to the bone. *Cancer Res* 2007;**67**(8):3524–8.
16. Bäuerle T, Adwan H, Kiessling F, et al. Characterization of a rat model with site-specific bone metastasis induced by MDA-MB-231 breast cancer cells and its application to the effects of an antibody against bone sialoprotein. *Int J Cancer* 2005;**115**(2):177–86.
17. Brix G, Semmler W, Port R, et al. Pharmacokinetic parameters in CNS Gd-DTPA enhanced MR imaging. *J Comput Assist Tomogr* 1991;**15**(4):621–8.
18. Herneth AM, Guccione S, Bednarski M. Apparent diffusion coefficient: a quantitative parameter for *in vivo* tumor characterization. *Eur J Radiol* 2003;**45**(3):208–13.
19. Kiessling F, Jugold M, Woenne EC, Brix G. Non-invasive assessment of vessel morphology and function in tumors by magnetic resonance imaging. *Eur Radiol* 2007;**17**(8):2136–48.
20. Benjamin LE, Golijanin D, Itin A, Pode D, Keshet E. Selective ablation of immature blood vessels in established human tumors follows vascular endothelial growth factor withdrawal. *J Clin Invest* 1999;**103**(2):159–65.
21. Andersen TL, Sondergaard TE, Skorzynska KE, et al. A physical mechanism for coupling bone resorption and formation in adult human bone. *Am J Pathol* 2009;**174**(1):239–47.
22. Luckman SP, Hughes DE, Coxon FP, et al. Nitrogen-containing bisphosphonates inhibit the mevalonate pathway and prevent post-translational prenylation of GTP-binding proteins, including Ras. *J Bone Miner Res* 1998;**13**(4):581–9.
23. Peng H, Sohara Y, Moats RA, et al. The activity of zoledronic acid on neuroblastoma bone metastasis involves inhibition of osteoclasts and tumor cell survival and proliferation. *Cancer Res* 2007;**67**(19):9346–55.
24. Strube A, Hoffmann J, Stepina E, et al. Sagopilone inhibits breast cancer bone metastasis and bone destruction due to simultaneous inhibition of both tumor growth and bone resorption. *Clin Cancer Res* 2009;**15**(11):3751–9.
25. Belotti D, Vergani V, Drudis T, et al. The microtubule-affecting drug paclitaxel has antiangiogenic activity. *Clin Cancer Res* 1996;**2**(11):1843–9.
26. Schwartz EL. Antivascular actions of microtubule-binding drugs. *Clin Cancer Res* 2009;**15**(8):2594–601.
27. Miller K, Wang M, Gralow J, et al. Paclitaxel plus bevacizumab versus paclitaxel alone for metastatic breast cancer. *New Engl J Med* 2007;**357**(26):2666–76.
28. Naumova E, Ubezio P, Garofalo A, et al. The vascular targeting property of paclitaxel is enhanced by SU6668, a receptor tyrosine kinase inhibitor, causing apoptosis of endothelial cells and inhibition of angiogenesis. *Clin Cancer Res* 2006;**12**(6):1839–49.
29. Jain RK. Normalization of tumor vasculature: an emerging concept in antiangiogenic therapy. *Science* 2005;**307**(5706):58–62.